Aggregation Behaviour of Synthetic Peptide Surfactants †

By Yukito Murakami,* Akio Nakano, Kiyoshi Iwamoto, and Akira Yoshimatsu, Department of Organic Synthesis, Faculty of Engineering, Kyushu University, Fukuoka 812, Japan

Single-chain surfactants with an amino-acid residue as part of a hydrophobic chain, *SS'*-bis-[*N*-dodecyl-N^{α}-(6-trimethylammoniohexanoyl)-L-hemicysteinamide] bromide [$(N^{+}C_5CysC_{12})_2$], *N*-dodecyl-N^{α}-(6-trimethylammoniohexanoyl)-*S*-benzyl-L-cysteinamide bromide [$N^{+}C_5Cys(Bzl)C_{12}$], and *N*-dodecyl-N^{α}-(6-trimethylammoniohexanoyl)-L-aspartamide bromide ($N^{+}C_5AspC_{12}$) have been synthesized and the structures of the aggregates formed in aqueous media investigated. The peptide surfactants form tighter aggregates than ordinary micelles formed with octadecyltrimethylammonium chloride. The weight-average molecular weights of the aggregates in aqueous media were determined by the low angle laser light scattering technique: $N^{+}C_5Cys(Bzl)C_{12}$, 7.04×10^6; $(N^{+}C_5CysC_{12})_2$, 1.49×10^6; $N^{+}C_5AspC_{12}$, 5.06×10^4. Consequently, $N^{+}C_5AspC_{12}$ forms tight spherical micelles while $(N^{+}C_5CysC_{12})_2$ and $N^{+}C_5Cys(Bzl)C_{12}$ constitute tight and large cylindrical micelles. This aggregation behaviour was also confirmed by electron microscopy. The introduction of an amino-acid residue into the hydrophobic chain of a surfactant results in tightening of the aggregate structure in aqueous media, probably due to intermolecular hydrogen bonding among amino-acid moieties in the micelle.

We have investigated the catalytic efficiency of synthetic peptide surfactants for the degradation of *p*-nitrophenyl carboxylates.[1] These peptide surfactants have an amino-acid residue as part of the hydrophobic chain and seem to have unique structural features in aqueous media, compared with ordinary micelles formed with hexadecyltrimethylammonium bromide (CTAB)

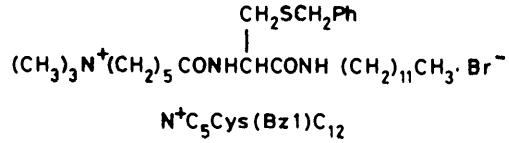

$N^{+}C_5Cys(Bzl)C_{12}$

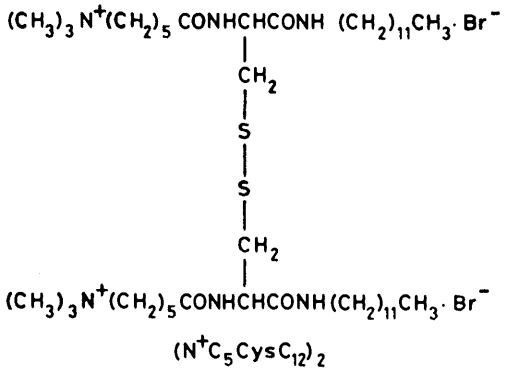

$(N^{+}C_5CysC_{12})_2$

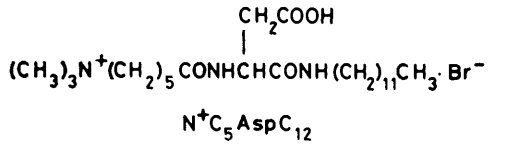

$N^{+}C_5AspC_{12}$

and octadecyltrimethylammonium chloride (STAC). We have no information as to the structures of the peptide surfactant aggregates formed in aqueous media, although the aggregate structure for CTAB micelle has been satisfactorily elucidated.[2] In this work, the aggregate structures of the peptide surfactants $N^{+}C_5Cys(Bzl)C_{12}$, $(N^{+}C_5CysC_{12})_2$, and $N^{+}C_5AspC_{12}$ were investigated by various physical methods, since the aggregation behaviour is of interest in connection with the chemistry of bioaggregates.[3]

† Preliminary account, Y. Murakami, A. Nakano, K. Iwamoto, and A. Yoshimatsu, *Chem. Letters*, 1979, 951.

EXPERIMENTAL

I.r. spectra were measured with a JASCO DS-403G grating spectrophotometer. ^{1}H N.m.r. spectra were taken on either a Varian A-60 or a Bruker WH-90 FT spectrometer with tetramethylsilane (in deuteriochloroform or deuteriomethanol) and 3-(trimethylsilyl)propanesulphonic acid (in deuterium oxide) as internal references. E.s.r. spectra were recorded at room temperature (22 °C) on a JEOL JES-ME-3 X-band spectrometer with manganese(II) ion diffused thermally into magnesium oxide as a reference. Weight-average molecular weights were determined by using a low angle laser light scattering photometer LS-8 (Toya Soda Manufacturing Co., Ltd.). Surface tension measurements were performed at room temperature with a Kyowa DIGI-O-MATIC ESB-IV electrosurface balance assembled by the Wilhelmy principle.

Electron Microscopy.—Samples for electron microscopy were prepared by sonicating aqueous surfactant solutions (10 mmol l^{-1}) containing 1.0% (w/w) uranyl acetate for 2 min at 30 W power (model W-220F; Heat Systems-Ultrasonics, Inc.). A drop of the solution was applied to a carbon grid, which was then placed in a vacuum desiccator. Electron micrographs were taken on a JEOL JEM-100CX electron microscope.

Octadecyltrimethylammonium chloride (STAC) (Ishizu Pharmaceutical Co.) was recrystallized from aqueous ethanol; no definite m.p., softens at 80 °C, and decomposes above 180 °C.[4] 4-Hydroxy-2,2,6,6-tetramethylpiperidine 1-oxyl (1) was prepared according to the procedure by Weiner,[5] m.p. 71—73 °C (lit.,[5] 70—71 °C). 4-(Cyclohexylacetoxy)-2,2,6,6-tetramethylpiperidine 1-oxyl (2) was prepared by the reaction of cyclohexylacetyl chloride with (1).[6] 2-(8-*Carboxyoctyl*)-5,5-*dimethyl*-2-*octyl*-3-*oxazolidine* 1-*oxyl* (3) was synthesized in a manner similar to that reported by McConnell *et al.* for the preparation of 2-(6-carboxyhexyl)-5,5-dimethyl-2-octyl-3-oxazolidine 1-oxyl.[7] It

was a viscous orange liquid, $\nu_{max.}$ (neat) 2 820 and 2 760 (CH) and 1 690 cm^{-1} (C=O) (Found: C, 68.45; H, 11.0; N, 3.7. $C_{22}H_{42}NO_4$ requires C, 68.7; H, 11.0; N, 3.65%). The synthesis of *N*-dodecyl-*N*$^{\alpha}$-(6-trimethylammoniohexanoyl)-*S*-benzyl-L-cysteinamide bromide [$N^+C_5Cys(Bzl)C_{12}$] was reported previously.[1b]

SS'-*Bis*-[N-*dodecyl*-N$^{\alpha}$-(6-*trimethylammoniohexanoyl*)-L-*hemicysteinamide*] *Bromide* [$(N^+C_5CysC_{12})_2$].—An analytically pure sample of *N*-dodecyl-*N*$^{\alpha}$-(6-trimethylammoniohexanoyl)-L-cysteinamide bromide [1b] was dissolved in methanol, and air was bubbled through the solution until the nitroprusside test for the solution was negative. After complete oxidation, methanol was evaporated off *in vacuo* to give a solid in quantitative yield, m.p. 157—165 °C; nitroprusside test, negative; Ellman test, negative.

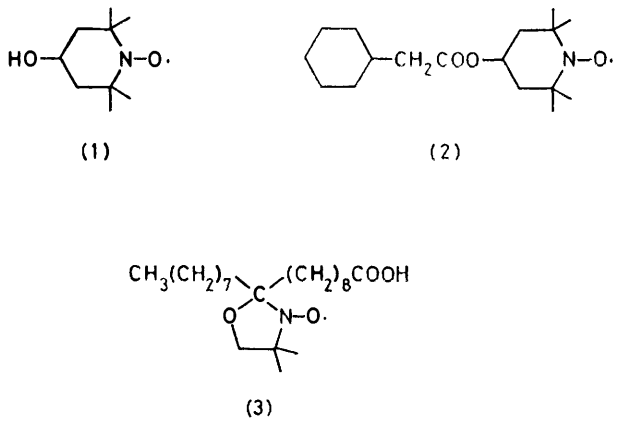

The synthetic procedure for *N*-dodecyl-*N*$^{\alpha}$-(6-trimethylammoniohexanoyl)-L-aspartamide bromide ($N^+C_5AspC_{12}$) is outlined in the Scheme.

N-*Dodecyl*-N$^{\alpha}$-*t-butoxycarbonyl*-O-*benzyl*-L-*aspartamide* (4).—To a solution of *N*-t-butoxycarbonyl-*O*-benzylaspartic acid [8] (10.0 g, 0.03 mol) in dry dichloromethane (40 ml) was added dicyclohexylcarbodi-imide (6.4 g, 0.03 mol) with stirring at 0 °C. After 10 min, 1-aminododecane (5.4, g 0.03 mol) was added to the solution and the mixture was stirred for 3 h at 0 °C and for a further 12 h at room temperature. The solvent was evaporated off *in vacuo* and the residue was suspended in chilled ethyl acetate. A precipitate (*NN'*-dicyclohexylurea) was removed by filtration and the filtrate was washed with saturated aqueous sodium chloride, 10% aqueous citric acid, saturated aqueous sodium chloride, 4% aqueous sodium hydrogencarbonate, and saturated aqueous sodium chloride in this sequence. After drying (Na_2SO_4), the mixture was evaporated *in vacuo* to give an oil which was subsequently solidified by treatment with n-hexane. Recrystallization from n-hexane afforded a powder (13.0 g, 86%), m.p. 52.5—55.0 °C; $\nu_{max.}$ (KBr) 3 360 (NH), 2 950 and 2 860 (CH), and 1 740 and 1 660 cm^{-1} (C=O); $\delta(CDCl_3)$ 0.88 [3 H, t, $CH_3(CH_2)_{11}$], 1.25 [20 H, s, $CH_3(CH_2)_{10}CH_2$], 1.45 [9 H, s, $(CH_3)_3C$], 2.88 (2 H, d, CH_2-$COOCH_2Ph$), 4.57br [1 H, t, $CH(CH_2COOCH_2Ph)$], 3.21 (2 H, t, NH_2CH_2), 5.15 (2 H, s, $COOCH_2$ Ph), and 7.37 (5 H, s, phenyl H).

N-*Dodecyl*-N$^{\alpha}$-(6-*bromohexanoyl*)-O-*benzyl*-L-*aspartamide* (6).—Trifluoroacetic acid (25.0 g) was added to a dichloromethane solution (17 ml) of (4) (3,2 g, 6.5 mmol) and the mixture was stirred for 1 h at room temperature. Evaporation of excess of trifluoroacetic acid *in vacuo* below 40 °C gave an oil (5) (3.3 g, quantitative). Elimination of the t-butoxycarbonyl group was confirmed by n.m.r. spectroscopy. The amine (5) (3.3 g, 6.5 mmol) and triethylamine (2.0 g, 20 mmol) were dissolved in dichloromethane (20 ml) and the solution was cooled to 0 °C. 6-Bromohexanoyl chloride (2.8 g, 13 mmol) dissolved in dichloromethane (15 ml) was added dropwise to the solution at 0 °C with stirring. The mixture was further stirred for 2 h at room temperature and then washed with 5% aqueous hydrogencarbonate (50 ml × 2), saturated aqueous sodium chloride (50 ml), 5% aqueous citric acid (50 ml), and saturated aqueous sodium chloride (50 ml) in this sequence. After drying (Na_2SO_4), the mixture was evaporated *in vacuo* at 40 °C to give a solid which was recrystallized from light petroleum–n-hexane as a powder (3.6 g, 97%), m.p. 59.5—61.0 °C; $\nu_{max.}$ (KBr) 3 380 (NH), 2 960 and 2 900 (CH), and 1 742 and 1 660 cm^{-1} (C=O); $\delta(CDCl_3)$ 0.88br [3 H, t, $CH_3(CH_2)_{11}$], 1.26 [20

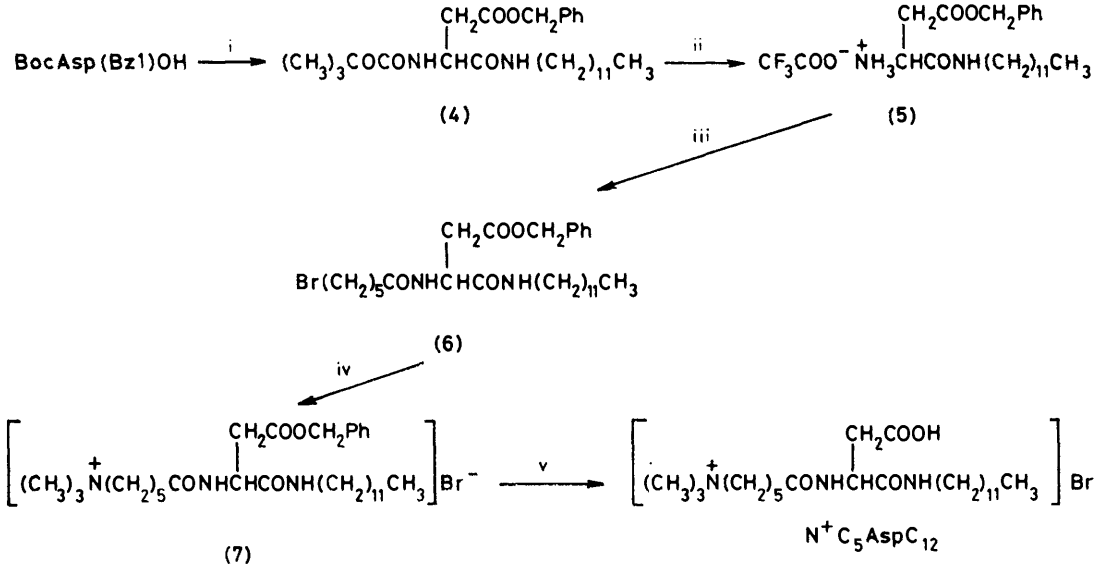

SCHEME *Reagents:* i, $NH_2[CH_2]_{11}CH_3$–dicyclohexylcarbodi-imide; ii, CF_3CO_2H; iii, $Br[CH_2]_5COCl$; iv, $(CH_3)_3N$; v, H_2–Pd

H, s, $CH_3(CH_2)_{10}CH_2$], *ca.* 2.00 [6 H, m, $BrCH_2(CH_2)_3CH_2$], 2.23br [2 H, t, $BrCH_2(CH_2)_3CH_2$], 2.84 (2 H, d, CH_2COOCH_2-Ph), 3.25 [2 H, t, $NHCH_2(CH_2)_{10}CH_3$], 3.37 (2 H, t, $BrCH_2$), 4.85br [1 H, t, $CH(CH_2COOCH_2Ph)$], 5.16 (2 H, s, $COOCH_2$-Ph), and 7.38 (5 H, s, phenyl H).

N-Dodecyl-N$^{\alpha}$-(6-trimethylammoniohexanoyl)-O-benzyl-L-aspartamide Bromide (7).—Dry trimethylamine gas was introduced into a benzene solution (40 ml) of (6) (3.6 g, 5.7 mmol) for 3 h and the solution was stirred at room temperature for 14 h. After benzene was evaporated off *in vacuo*, the crude product was recrystallized twice from ethyl acetate (2.8 g, 71%), m.p. 115—117 °C; $\nu_{max.}$ (KBr) 3 280 (NH), 2 920 and 2 850 (CH), and 1 720, 1 640, and 1 540 cm^{-1} (C=O); $\delta(CDCl_3)$ 0.88br [3 H, t, $CH_3(CH_2)_{10}CH_2$], 1.25 [20 H, s, $CH_3(CH_2)_{10}CH_2$], *ca.* 2.00 [6 H, m, $(CH_3)_3N^+CH_2$-$(CH_2)_3CH_2$], 2,37br [2 H, t, $(CH_3)_3N^+CH_2(CH_2)_3CH_2$], 2.84—3.73 [6 H, m, CH_2COOCH_2Ph, $NHCH_2(CH_2)_{10}CH_3$, and $(CH_3)_3N^+CH_2(CH_2)_3CH_2$], 3.35 [9 H, s, $(CH_3)_3N^+$], 4.80br [1 H, t, $CH(CH_2COOCH_2Ph)$], 5.14 (2 H, s, $COOCH_2$-Ph), and 7.40 (5 H, s, phenyl H) (Found: C, 59.0; H, 9.0; N, 6.55. $C_{32}H_{56}BrN_3O_4 \cdot 3/2H_2O$ requires C, 58.8; H, 9.1; N, 6.45%).

N-Dodecyl-N$^{\alpha}$-(6-trimethylammoniohexanoyl)-L-aspartamide Bromide ($N^+C_5AspC_{12}$).—Hydrogen was bubbled for 25 h through a methanol solution (30 ml) of (7) (2.0 g, 3.2 mmol) in the presence of 10% palladium on charcoal (1.0 g). After the catalyst was removed by filtration through a column of Celite 545, the solvent was evaporated off *in vacuo*. The residue was recrystallized from acetonitrile to afford a powder (1.3 g, 78%), m.p. 151—153 °C, $[\alpha]_D^{20}$ −6.00° (*c* 3.23, ethanol); $\nu_{max.}$ (KBr) 3 340 (NH), 2 920 and 2 850 (CH), and 1 720, 1 640, and 1 530 cm^{-1} (C=O); $\delta([^2H_4]$-methanol) 0.89br [3 H, t, $CH_3(CH_2)_{10}$], 1.30 [20 H, s, CH_3-$(CH_2)_{10}$], *ca.* 2.10 [6 H, m, $(CH_3)_3N^+CH_2(CH_2)_3CH_2$], 2.33br [2 H, t, $(CH_3)_3N^+CH_2(CH_2)_3CH_2CO$], 2.65—3.00 [6 H, m, $CHCH_2COOH$, $NHCH_2(CH_2)_{10}CH_3$, and $(CH_3)_3N^+CH_2$], 3.19 [9 H, s, $(CH_3)_3N^+$], and 4.75 (1 H, m, $CHCH_2COOH$) (Found: C, 55.75; H, 9.35; N, 7.95. $C_{25}H_{50}BrN_3O_4$ requires C, 55.95; H, 9.4; N, 7.85%).

RESULTS AND DISCUSSION

Evaluation of Molecular Motions by ^1H N.m.r. Method.—The c.m.c. values for the peptide surfactants and STAC are summarized in Table 1. The n.m.r. spectra were measured in deuterium oxide and $[^2H_4]$methanol at 36 °C. All the proton signals, the methylene signals in particular, for the peptide surfactants measured in deuterium oxide were considerably broadened relative to those obtained in $[^2H_4]$methanol. It should be noted that the methylene signals for $N^+C_5Cys(Bzl)C_{12}$ in deuterium oxide were too broad to evaluate their line width accurately. The broadening of signals seems to be caused by the slow translational and rotational motions of the molecules due to the formation of aggregates in aqueous media. The line widths indicate that the molecular motions of the alkyl chains of the peptide surfactants are more severely restricted than those of STAC in aqueous media.

TABLE 1

C.m.c. values of the surfactants at room temperature

Surfactant	C.m.c. (mol l^{-1})
$N^+C_5Cys(Bzl)C_{12}$	2.0×10^{-5} [a]
$(N^+C_5CysC_{12})_2$	1.1×10^{-5} [a]
$N^+C_5AspC_{12}$	2.0×10^{-4} [b]
STAC	3.4×10^{-4} [c]

[a] Surface tension method: pH 7.21 (borate–phosphate buffer), μ 0.10 (KCl). [b] Kinetic method; pH 7.62 (borate–phosphate buffer), μ 0.10 (KCl), in ethanol–dioxan–water (10.8 : 1 : 88.2 v/v); our unpublished data. [c] P. F. Grieger and C. A. Kraus, *J. Amer. Chem. Soc.*, 1948, **70**, 3803.

Spin Probe Method for Evaluation of Molecular Association.—In order to investigate the structures of aggregates associated with the mobility of solubilizates (spin probes) and the nature of the microenvironments, where the solubilizates are located, the e.s.r. technique was employed. 4-Hydroxy-2,2,6,6-tetramethylpiperidine 1-oxyl (1), 4-(cyclohexylacetoxy)-2,2,6,6-tetramethylpiperidine 1-oxyl (2), and 2-(8-carboxyoctyl)-5,5-dimethyl-2-octyl-3-oxazolidine 1-oxyl (3) were used as hydrophilic, relatively hydrophobic, and strongly hydrophobic spin probes, respectively.

The e.s.r. spectra of the hydrophilic spin probe (1) were taken in the peptide surfactant solutions and some organic solvents, and the e.s.r. parameters are summarized in Table 2. The $\bar{A}$ values obtained in the peptide surfactant solutions are larger than that obtained in water. The result suggests that (1) is incorporated into a polar electrostatic layer and its molecular motion is not restricted at all. A rotational correlation time (τ_c) was calculated by the equation, $\tau_c = A\Delta H_{(m=+1)} \times [(I_{(m=+1)}/I_{(m=-1)})^{1/2} - 1]$.[9] The τ_c values also confirm this conclusion.

The e.s.r. spectrum of (2) in aqueous $(N^+C_5CysC_{12})_2$ solution is shown in Figure 1(A); the high-field line is resolved into two. This phenomenon was observed for the phospholipid bilayer system by using 2,2,6,6-tetramethylpiperidine 1-oxyl as a probe.[10] Signal P arises from (2) dissolved in an electrostatic phase and signal H is due to the spin probe placed in a hydrophobic environment. The spectral parameter *f*, equal to H/(H + P), shows approximately the fraction of the spin-labelled probe placed in the hydrophobic region of the aggregates.[10] The *f* values for the $(N^+C_5CysC_{12})_2$ and N^+C_5-$AspC_{12}$ systems are 0.42 and 0.18, respectively. Two apparent $\bar{A}$ values, $\bar{A}$(hyd) and $\bar{A}$(el), were evaluated directly from the spectra. $\bar{A}$(hyd) is a hyperfine coupling constant for the component incorporated into the hydrophobic region of the aggregates, whilst $\bar{A}$(el) is that for the component located in the electrostatic phase. The $\bar{A}$(hyd) values obtained indicate that the hydro-

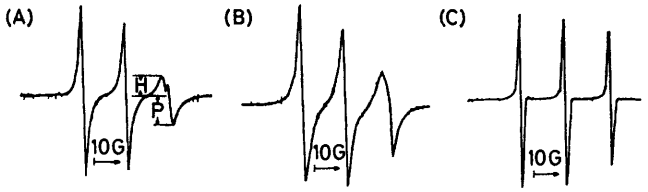

FIGURE 1 E.s.r. spectra of (2) in $(N^+C_5CysC_{12})_2$ solution (A), STAC solution (B), and ethanol (C); refer to Table 4 for experimental conditions

TABLE 2

E.s.r. spectral data for (1) (5.40×10^{-4} mol l^{-1}) at room temperature (22 °C)

Surfactant (S)	10^2 [S]/mol l^{-1}	Medium	$\bar{A}$/G	$10^{10}\tau_c$/s
$N^+C_5Cys(Bzl)C_{12}$	1.03	*a*	17.23	0.51
$(N^+C_5CysC_{12})_2$	1.03	*a*	17.25	0.51
$N^+C_5AspC_{12}$	0.99	*a*	17.13	0.45
STAC	1.06	*a*	17.19	0.54
		a	17.10	0.45
		Methanol [b]	16.31	0.25
		Acetonitrile [b]	15.81	0.24
		Benzene [b]	15.63	0.12

[a] Ethanol–water (1 : 99 v/v); pH 6.53, μ 0.10 (KCl). [b] Contains 1.0% (v/v) ethanol.

phobic environment for (2) corresponds to that provided by acetonitrile. A fraction of (2) seems to be placed at the electrostatic layer which yields an environment more polar than in water. In STAC and $N^+C_5Cys(Bzl)C_{12}$ solutions, only the line broadening was observed. Judging from their $\bar{A}$ values, (2) is placed primarily in the electrostatic region of the aggregates (Table 3).

TABLE 3

E.s.r. spectral data for (2) (5.25×10^{-4} mol l^{-1}) at room temperature (22 °C)

Surfactant (S)	10^2 [S]/mol l^{-1}	Medium	$\bar{A}$/G	$10^{10}\tau_c$/s
$N^+C_5Cys(Bzl)C_{12}$	0.99	*a*	16.99	1.89
$(N^+C_5CysC_{12})_2$	1.07	*a*	$\bar{A}$(el) 17.11, $\bar{A}$(hyd) 15.84	
$N^+C_5AspC_{12}$	0.99	*a*	$\bar{A}$(el) 17.09, $\bar{A}$(hyd) 15.57	
STAC	1.05	*a*	16.82	6.80
		a	(17.01) [c]	1.25
		Methanol [b]	16.15	0.26
		Acetonitrile [b]	15.79	0.31
		Benzene [b]	15.56	0.40

[a] Ethanol–water (1 : 99 v/v); pH 6.53, μ 0.10 (KCl). [b] Contains 1.0% (v/v) ethanol. [c] Slightly turbid.

The e.s.r. spectra of (3) measured in the peptide surfactant solutions were different from those in aqueous STAC and organic solvents, and quite similar to those observed in bilayer membranes.[11] The motion-averaged hyperfine splittings, $\bar{A}_\parallel$ and $\bar{A}_\perp$, were estimated, and the motion independent $\bar{A}$ parameter was calculated by the equation $\bar{A} = 1/3(\bar{A}_\parallel + 2\bar{A}_\perp)$.[12] On the other hand, only the line broadening was observed for the e.s.r. signals of (3) in aqueous STAC. In such a case, an isotropic hyperfine splitting constant ($\bar{A}$) was obtained by dividing the difference between the high-field and low-field lines by two. The e.s.r. parameters for (3) are summarized in Table 4. It has been known that the value of τ_c increases in general as the value of $|\bar{A}_\parallel - \bar{A}_\perp|$ increases. Thus, the magnitude of τ_c decreases in the sequence, $N^+C_5Cys(Bzl)C_{12} > (N^+C_5CysC_{12})_2 > N^+C_5AspC_{12} \gg$ STAC. The result indicates that the molecular motion of (3) is severely restricted (anisotropic immobilization) only in these peptide surfactant systems. In other words, peptide surfactants must form aggregates tighter than ordinary micelles in aqueous media. The hyperfine splitting constant of the nitroxide radicals is rather sensitive to the change in solvent polarity and in general has a linear correlation with the Dimroth–Reichardt E_T (30) parameter.[13] In fact, this correlation is observed as shown in Figure 2. The $\bar{A}$ values for (3) obtained in the peptide surfactant solutions are smaller than that observed in STAC solution except for that evaluated in $N^+C_5Cys(Bzl)C_{12}$ solution. This indicates that the oxazolidine ring of (3) is incorporated tightly into the hydrophobic region of the aggregates of $(N^+C_5CysC_{12})_2$ and $N^+C_5AspC_{12}$. On the other hand, the bulky benzyl group seems to perturb the aggregate structure of $N^+C_5Cys(Bzl)C_{12}$ so as to incorporate water molecules into the hydrophobic core to a greater extent than the other peptide surfactants. Figure 2 shows that the microenvironment of N^+C_5Asp-

TABLE 4

E.s.r. spectral data for (3) (5.66×10^{-4} mol l^{-1}) at room temperature (22 °C)

Surfactant (S)	10^2 [S]/mol l^{-1}	Medium	$\bar{A}_\parallel$/G	$\bar{A}_\perp$/G	$\bar{A}$/G	$10^{10}\tau_c$/s
$N^+C_5Cys(Bzl)C_{12}$	1.04	*a*	26.07	9.80	15.22	
$(N^+C_5CysC_{12})_2$	1.06	*a*	24.11	10.13	14.79	
$N^+C_5AspC_{12}$	1.11	*a*	23.98	10.15	14.76	
$N^+C_5AspC_{12}$	3.70	*b*			14.57	25.54
STAC	1.14	*a*			15.15	15.50
STAC	3.70	*c*			15.00	12.70
		a,*d*			(15.90)	
		Methanol [e]			14.88	1.51
		Acetonitrile [e]			14.65	0.72
		Benzene [e]			14.33	1.08
		Nujol [e]			13.21	29.05

[a] Ethanol–water (1 : 99 v/v); pH 6.53, μ 0.10 (KCl). [b] Ethanol–water (11 : 89 v/v); pH 6.40, μ 0.10 (KCl). [c] Ethanol–water (11 : 89 v/v); pH 7.00, μ 0.10 (KCl). [d] Concentration of (3) 6.23×10^{-5} mol l^{-1}. [e] Contains 1.0% (v/v) ethanol. [f] Slightly turbid.

C_{12} for the oxazolidine ring of (3) corresponds to that provided by acetonitrile. The carboxy-group of $N^+C_5AspC_{12}$ seems to participate in the intermolecular hydrogen bonding to tighten the micellar structure and, consequently, water molecules are expelled from the hydrophobic region. In conclusion, (3) is completely incorporated into the peptide surfactants and anisotropic immobilization is exercised. On the other hand, (2) is distributed between the hydrophobic region and the electrostatic layer of the aggregates without rapid exchange between the species placed in the different environments. All the results also suggest that the peptide surfactants may form tighter aggregates than the ordinary micelles in aqueous media.

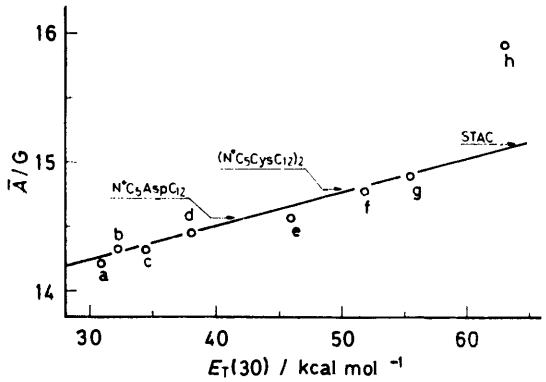

FIGURE 2 Correlation of nitrogen hyperfine splitting constant ($\bar{A}$) for (3) with the Dimroth–Reichardt parameter: a, hexane; b, carbon tetrachloride; c, benzene; d, ethyl acetate; e, acetonitrile; f, ethanol; g, methanol; h, water

basis of their molecular weights and aggregation numbers. Tanford postulated the maximum allowable aggregation number for the formation of globular micelles by using two parameters,[16] the volume occupied by an alkyl chain with C_n carbon atoms, embedded in the hydrophobic core, and the maximum length for the alkyl chain. By referring to his theory, the maximum aggregation numbers for spherical and ellipsoidal (oblate, $a_0/b_0 = 2$: a_0, size of a major semiaxis; b_0, size of a minor semiaxis) micelles are estimated to be 170 and 682, respectively, for C_n of 22. On the basis of these values, $N^+C_5AspC_{12}$ forms the spherical micelle while $N^+C_5Cys(Bzl)C_{12}$ and $(N^+C_5CysC_{12})_2$ form larger cylindrical aggregates even below the concentration range used for electron microscopy and e.s.r. measurements (10^{-2} mol l^{-1}). This conclusion is consistent with the literature data summarized by Thomas *et al.*[17] The cylindrical aggregate of CTAB appears in water in the concentration range above 2.55 $\times$ 10^{-1} mol l^{-1}.[18]

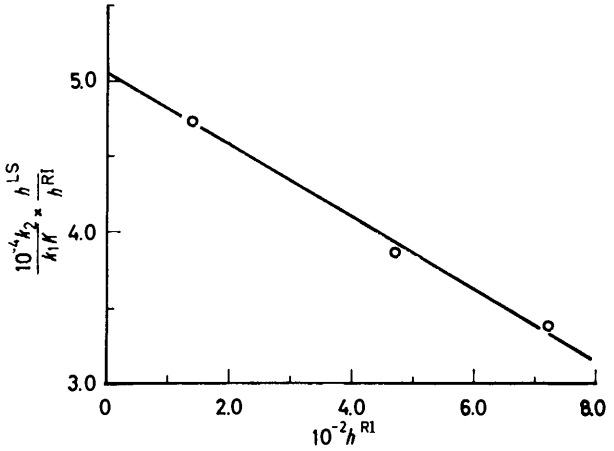

FIGURE 3 Plot of two quantities on the basis of equation (1) for determination of the apparent molecular weight of $N^+C_5AspC_{12}$ aggregate in water at 25 °C: concentration range of $N^+C_5AspC_{12}$, 1.15×10^{-2}—2.45×10^{-3} mol l^{-1}

TABLE 5

Weight-average molecular weights ($\bar{M}$), aggregation number (N), and shapes of the aggregates of peptide surfactants measured in water at 25 °C

Surfactant	Concentration (mol l^{-1})	$\bar{M}$	N	Shape
$N^+C_5Cys(Bzl)C_{12}$	1.09×10^{-2}—2.42×10^{-3}	7.04×10^6	11 500	Cylindrical
$(N^+C_5CysC_{12})_2$	1.66×10^{-3}—1.96×10^{-4}	1.49×10^6	1 460	Cylindrical
$N^+C_5AspC_{12}$	1.15×10^{-2}—2.45×10^{-3}	5.06×10^4	94	Spherical

Molecular Weights and Shapes of the Aggregates.—The weight-average molecular weight ($\bar{M}$) of an aggregate can be evaluated by the low angle laser light scattering technique developed by Kaye *et al.*[14] The $\bar{M}$ value can be obtained from a plot of $(k_2/k_1K) \times (h^{LS}/h^{RI})$ against h^{RI} [equation (1) [15]] (see Appendix): h^{LS} and h^{RI} are the intensity of the scattering light and magnitude of the refractive index, respectively; k_2/k_1K inherent to the apparatus and measuring conditions is determined by using a reference material [poly(ethylene oxide); Toyo Soda RE-4; 14.8×10^4 g mol^{-1}].

$$\frac{k_2}{k_1K}\frac{h^{LS}}{h^{RI}} = \bar{M} - \frac{2A_2\bar{M}^2}{k_2} \cdot h^{RI} \qquad (1)$$

The linear correlation is shown in Figure 3 for $N^+C_5AspC_{12}$. The molecular weights for the surfactant aggregates and their aggregation numbers are summarized in Table 5. Shapes of the aggregates formed with the peptide surfactants may be predicted on the

Electron Micrographs of the Aggregates.—The electron micrographs were taken for the peptide surfactants with the solutions of original concentration of 10^{-2} mol l^{-1}. The cylindrical rod-like structures were observed for samples of $N^+C_5Cys(Bzl)C_{12}$ and $(N^+C_5CysC_{12})_2$ as shown in Figure 4. The thickness of these layers is estimated to be *ca.* 35 Å; the CPK space-filling molecular model of $N^+C_5Cys(Bzl)C_{12}$ shows the hydrophobic chain length excluding the tertiary ammonium group to be 28 Å. This implies that the alkyl chains of the surfactants overlap mutually in the cylindrical compartment so as to form tighter aggregates (Figure 5). On the other hand, no

structure was observed in the electron micrograph for the sample of STAC solution. These facts indicate that the peptide surfactants may form the cylindrical aggregates more easily than the ordinary cationic surfactants.

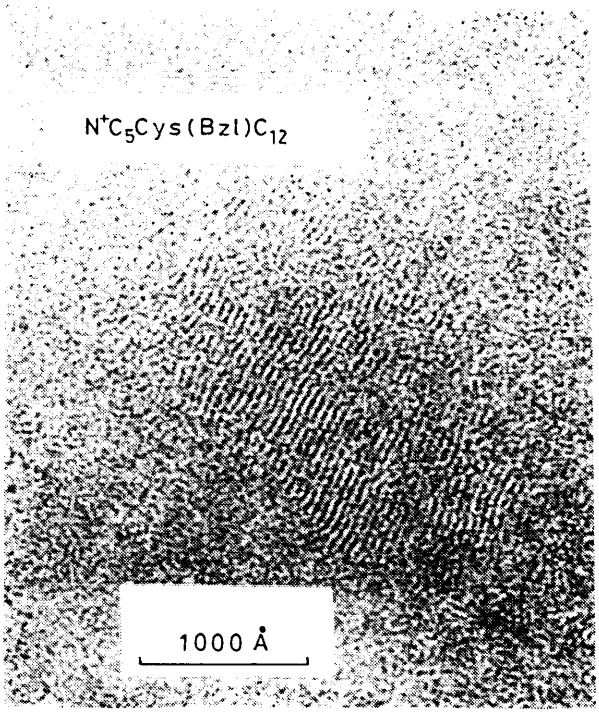

FIGURE 4 Electron micrograph for the aggregate of $N^+C_5Cys(Bzl)C_{12}$, magnification $\times 225\,000$

Conclusion.—The cationic peptide surfactants may form tighter and/or larger aggregates than the ordinary micelles formed with STAC and CTAB in a relatively low concentration range ($<10^{-2}$ mol l^{-1}). $N^+C_5AspC_{12}$ forms spherical micelles which are much tighter than the ordinary cationic ones. On the other hand, $N^+C_5Cys(Bzl)C_{12}$ and $(N^+C_5CysC_{12})_2$ constitute the larger aggregates of cylindrical structure. The introduction of an amino-acid residue into the hydrophobic chain of the

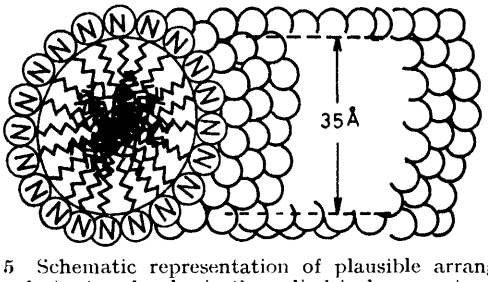

FIGURE 5 Schematic representation of plausible arrangement of surfactant molecules in the cylindrical compartment

surfactant molecules results in tightening of the aggregate structure in aqueous media. We suggest that intermolecular dipole–dipole interactions and/or intermolecular hydrogen bonding among the amide bonds located in the hydrophobic region of the aggregates play an important role in tightening the aggregate structure.

APPENDIX

In the light scattering method, Rayleigh's ratio R_θ is represented by equation (2) since the intramolecular interference function approaches unity as scattering angle θ is brought near to 0°; θ is set at 5° for LS-8. The other symbols are defined as follows: c, solute concentration

$$R_\theta = Kc\bar{M}(1 - 2A_2\bar{M}c) \quad (2)$$

$$K = 2\pi^2 n_0^2(\Delta n/c)^2(1 + \cos^2\theta)/N_A\lambda_0^4$$

(g ml^{-1}); n_0, refractive index of solvent; Δn, difference in refractive index between solution and solvent; λ_0, wavelength of incident beam *in vacuo* (cm); N_A, Avogadro's number; A_2, second virial coefficient. The intensity of scattering light (h^{LS}) is related to R_θ by equation (3), where k_1 isthe proportionality constant.

$$h^{LS} = k_1R_\theta \quad (3)$$

The magnitude of the refractive index (h^{RI}) of the same sample used for the light scattering measurements has a correlation with c as shown by equation (4), where k_2 is the proportionality constant. Combination of equations (3)

$$h^{RI} = k_2c \quad (4)$$

and (4) with (2) gives equation (1).

We are indebted to Drs. K. Takeshita and I. Mochida, Research Institute of Industrial Science of Kyushu University, for the use of an electron microscope. We are also grateful to the Research Institute of Toyo Soda Manufacturing Co., Ltd. for providing the low angle laser light scattering photometer.

[0/324 *Received*, 28*th February*, 1980]

REFERENCES

[1] (*a*) Y. Murakami, A. Nakano, and K. Matsumoto, *Bull. Chem. Soc. Japan*, 1979, **52**, 2996; (*b*) Y. Murakami, A. Nakano, K. Matsumoto, and K. Iwamoto, *ibid.*, p. 3573.

[2] J. H. Fendler and E. J. Fendler, 'Catalysis in Micellar and Macromolecular Systems,' Academic Press, New York, 1975, p. 30.

[3] For example: G. H. Brown and J. J. Wolken, 'Liquid Crystals and Biological Structures,' Academic Press, New York, 1979.

[4] R. A. Reck, H. J. Harwood, and A. W. Ralston, *J. Org. Chem.*, 1947, **12**, 517.

[5] H. Weiner, *Biochemistry*, 1969, **8**, 526.

[6] Y. Murakami, A. Nakano, R. Miyata, and Y. Matsuda, *J.C.S., Perkin I*, 1979, 1669.

[7] W. L. Hubbell and H. M. McConnell, *J. Amer. Chem. Soc.*, 1971, **93**, 314.

[8] E. Bayer, G. Jung, and H. Hagenmaier, *Tetrahedron*, 1968, **24**, 4853.

[9] T. J. Stone, T. Buckman, P. L. Nordio, and H. M. McConnell, *Proc. Nat. Acad. Sci. U.S.A.*, 1965, **54**, 1010.

[10] E. J. Shimshick and H. M. McConnell, *Biochemistry*, 1973, **12**, 2351.

[11] W. L. Hubbel and H. M. McConnell, *Proc. Nat. Acad. Sci. U.S.A.*, 1969, **64**, 20.

[12] O. H. Griffith and P. C. Jost, 'Spin Labeling,' ed. L. T. Berliner, Academic Press, New York, 1976, ch. 12.

[13] B. R. Knauer and J. J. Napier, *J. Amer. Chem. Soc.*, 1976, **98**, 4395.

[14] (*a*) A. C. Ouano and W. Kaye, *J. Polymer Sci.*, 1974, **12**, 1151; (*b*) W. Kaye, A. J. Havlik, and J. B. McDaniel, *Polymer Letters*, 1971, **9**, 695.

[15] (*a*) B. H. Zimm, *J. Chem. Phys.*, 1948, **16**, 1093; (*b*) instruction manual for a low angle laser light scattering photometer model LS-8, Toyo Soda Manufacturing Co., Ltd., Tokyo, 1979.

[16] C. Tanford, *J. Phys. Chem.*, 1972, **76**, 3020.

[17] K. Kalyanasundaram, M. Grätzel, and J. K. Thomas, *J. Amer. Chem. Soc.*, 1975, **97**, 3915.

[18] P. Ekwall, L. Mandell, and P. Solyon, *J. Colloid. Interface Sci.*, 1971, **35**, 519.